

Supplement of Atmos. Chem. Phys., 17, 12533–12552, 2017  
<https://doi.org/10.5194/acp-17-12533-2017-supplement>  
© Author(s) 2017. This work is distributed under  
the Creative Commons Attribution 4.0 License.



*Supplement of*

## **Merged SAGE II, Ozone\_cci and OMPS ozone profile dataset and evaluation of ozone trends in the stratosphere**

**Viktorija F. Sofieva et al.**

*Correspondence to:* Viktorija F. Sofieva (viktorija.sofieva@fmi.fi)

The copyright of individual parts of the supplement might differ from the CC BY 4.0 License.

This supplement contains additional illustrations in support of the paper.

## 1 Intercomparison of deseasonalized anomalies from individual instruments

Figures S1-S7 show the deviations of the deseasonalized anomalies (in %) for individual instruments from the median deseasonalized anomalies of SAGE II, GOMOS, MIPAS, SCIAMACHY, OSIRIS, ACE-FTS and OMPS. In the beginning of SCIAMACHY and OMPS mission (Figs. S3 and S6, these periods are indicated by black dashed lines), significant deviations from the median anomaly are observed. SCIAMACHY and OMPS observations from these periods are not included in the merged dataset.

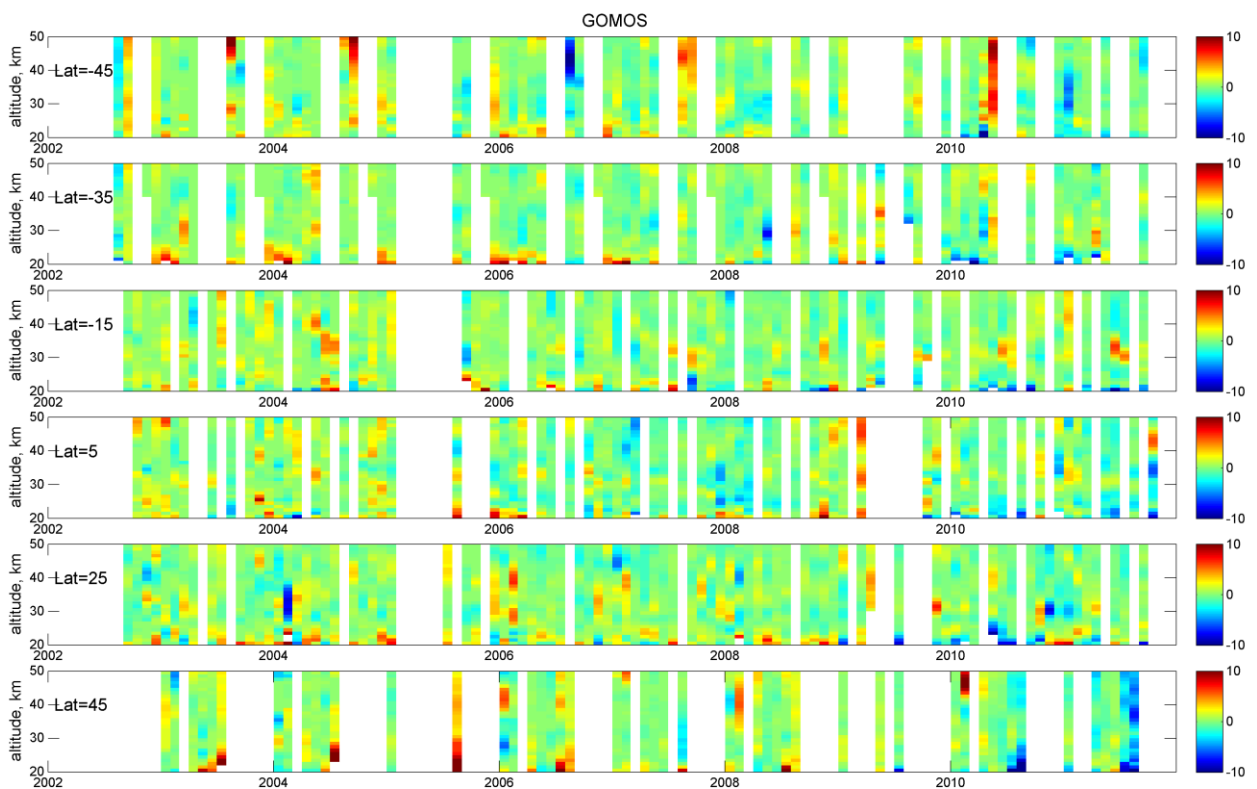


**Figure S1.** Deviations (in %, color) of GOMOS deseasonalized anomalies from the median deseasonalized anomalies of SAGE II, GOMOS, MIPAS, SCIAMACHY, OSIRIS, ACE-FTS and OMPS. 10°latitude bands are indicated by their centers in the panels.

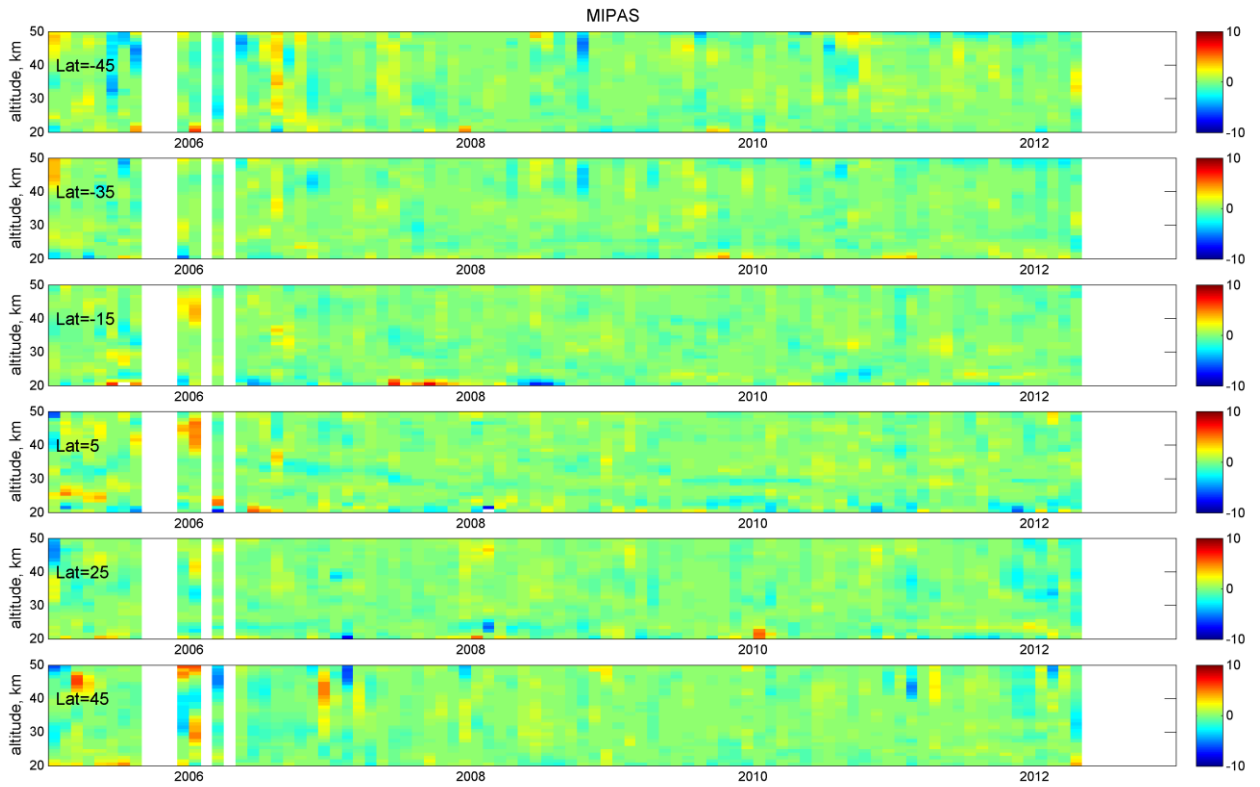


**Figure S2.** As Fig. S1, but for the MIPAS deseasonalized anomalies.

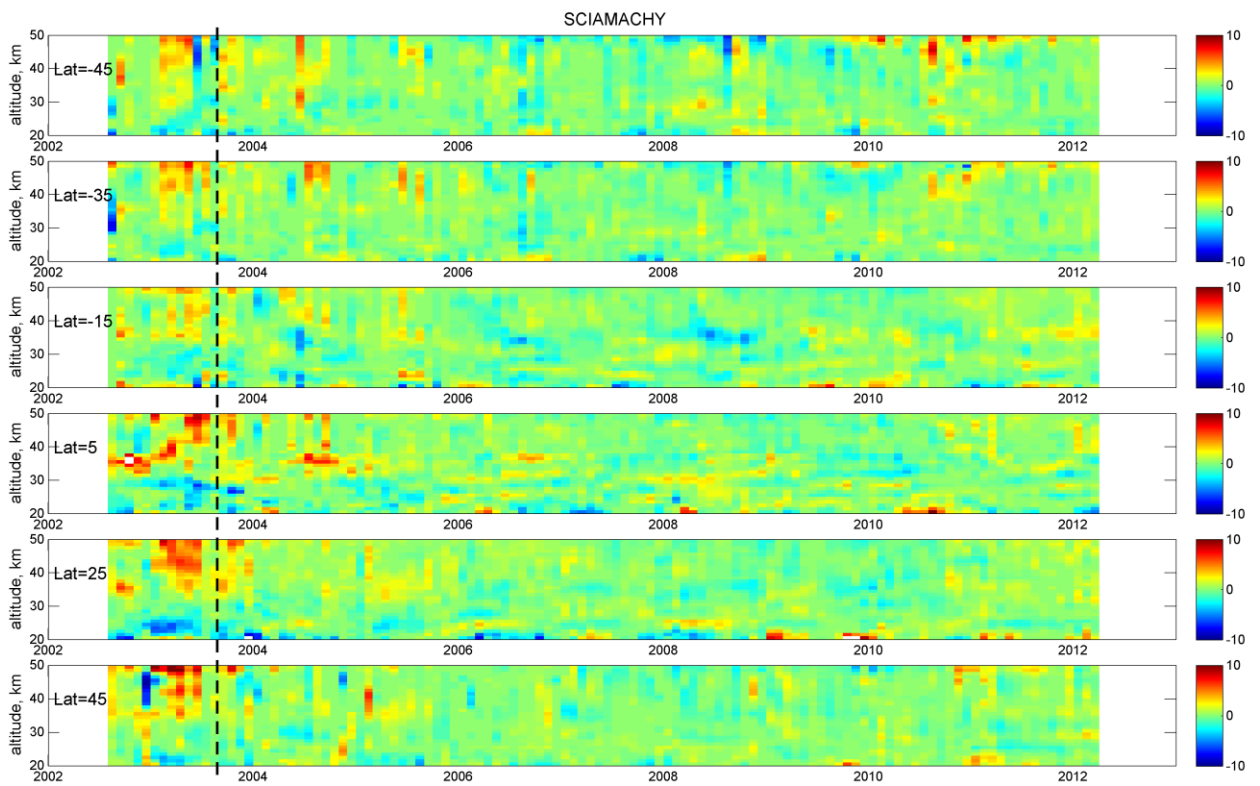


**Figure S3.** As Fig. S2, but for the SCIAMACHY deseasonalized anomalies. The dashed line indicates the beginning of the mission when significant deviations from the median deseasonalized anomalies are observed. These data from the beginning of the mission are not used for the merged dataset.

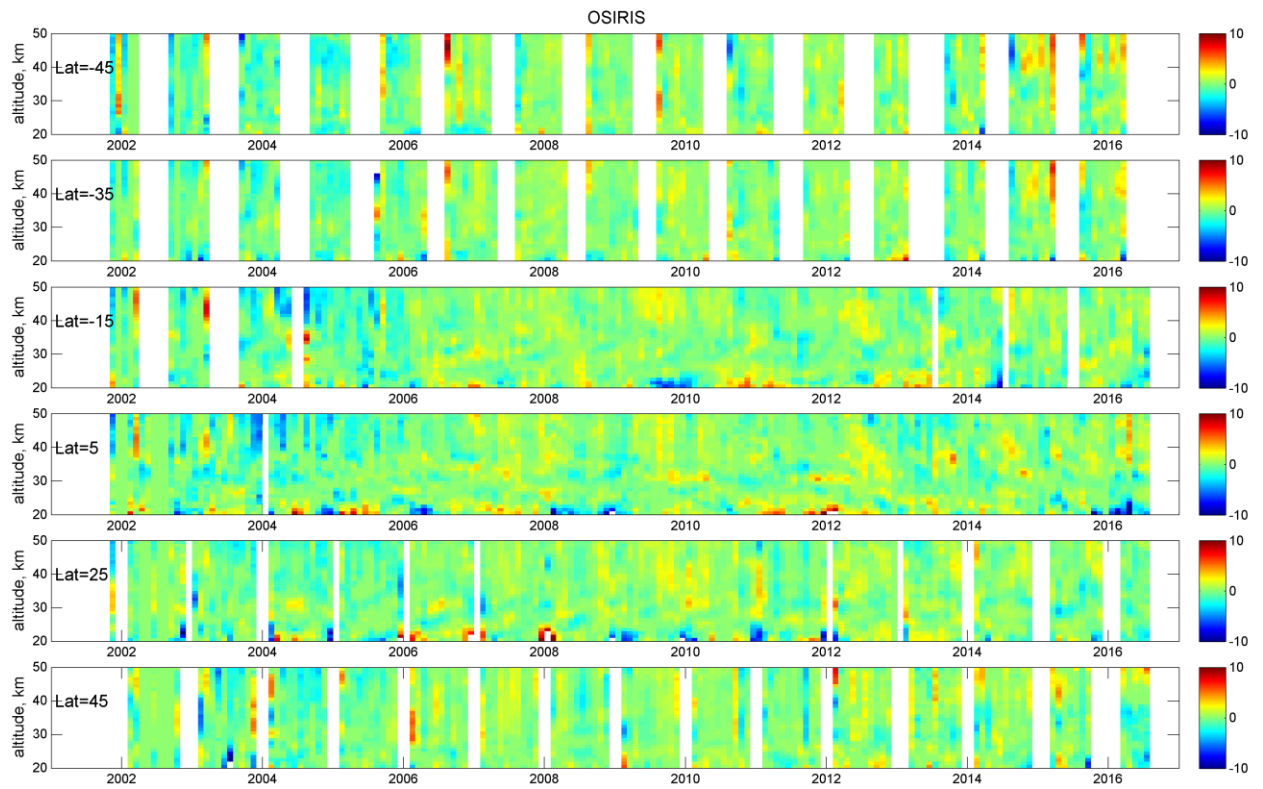


Figure S4. As Fig. S1, but for the OSIRIS deseasonalized anomalies.

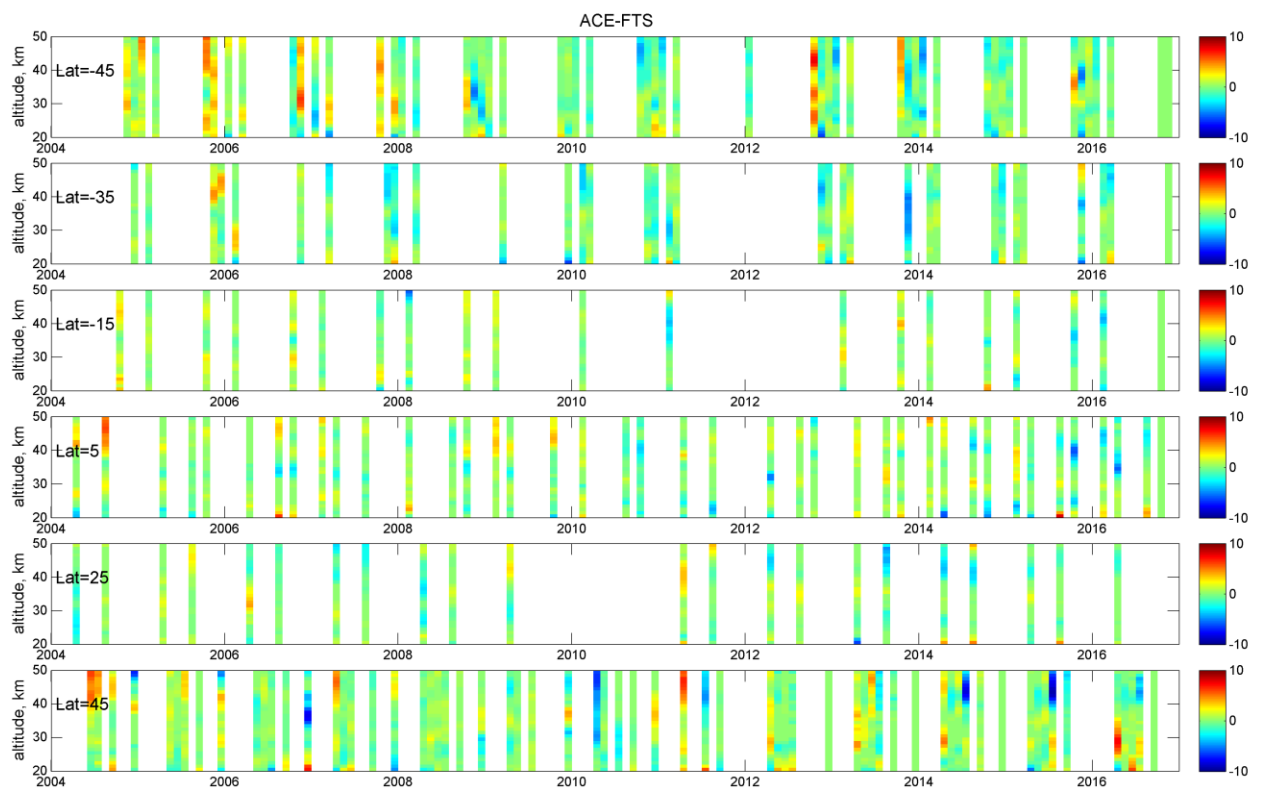


Figure S5. As Fig. S1, but for the ACE-FTS deseasonalized anomalies.

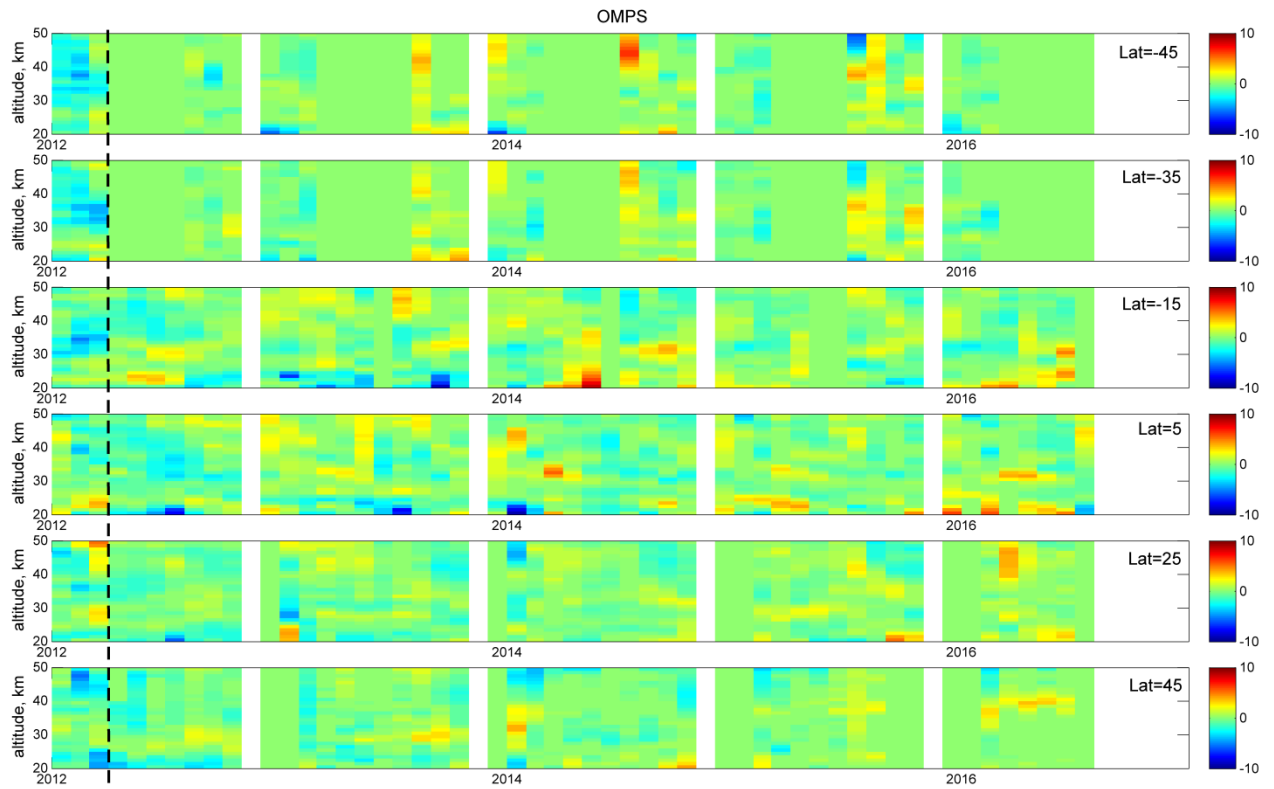


Figure S6. As Fig. S3, but for the OMPS deseasonalized anomalies.

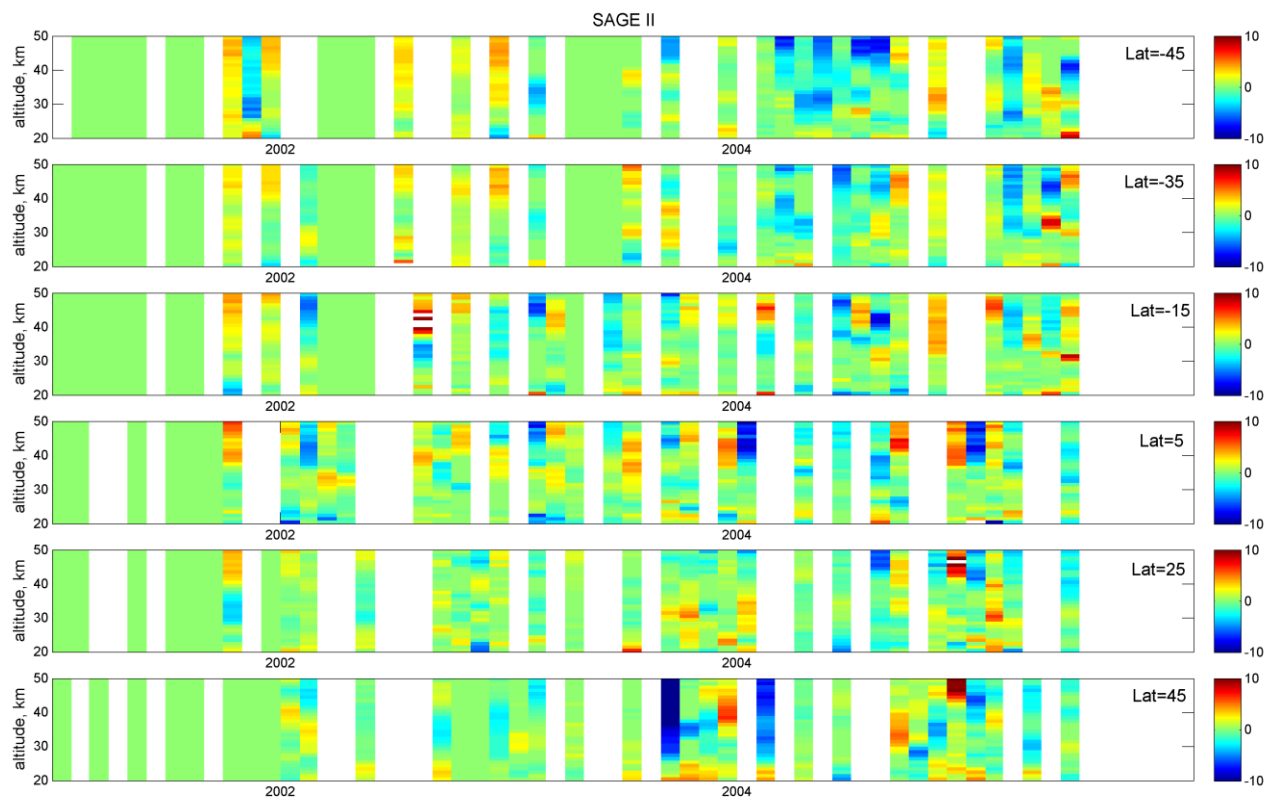


Figure S7. As Fig. S1, but for the SAGE II deseasonalized anomalies.

## 2 Representativeness of individual datasets in the merged dataset

The deseasonalized anomalies from individual dataset are usually very close to each other, so that several values can be typically found within the uncertainty interval of the merged anomaly  $\Delta_{merged} \pm \sigma_{\Delta_{merged}}$ . This is illustrated in Fig. S8, where the instruments having data within  $\Delta_{merged} \pm \sigma_{\Delta_{merged}}$  are indicated by colored markers.

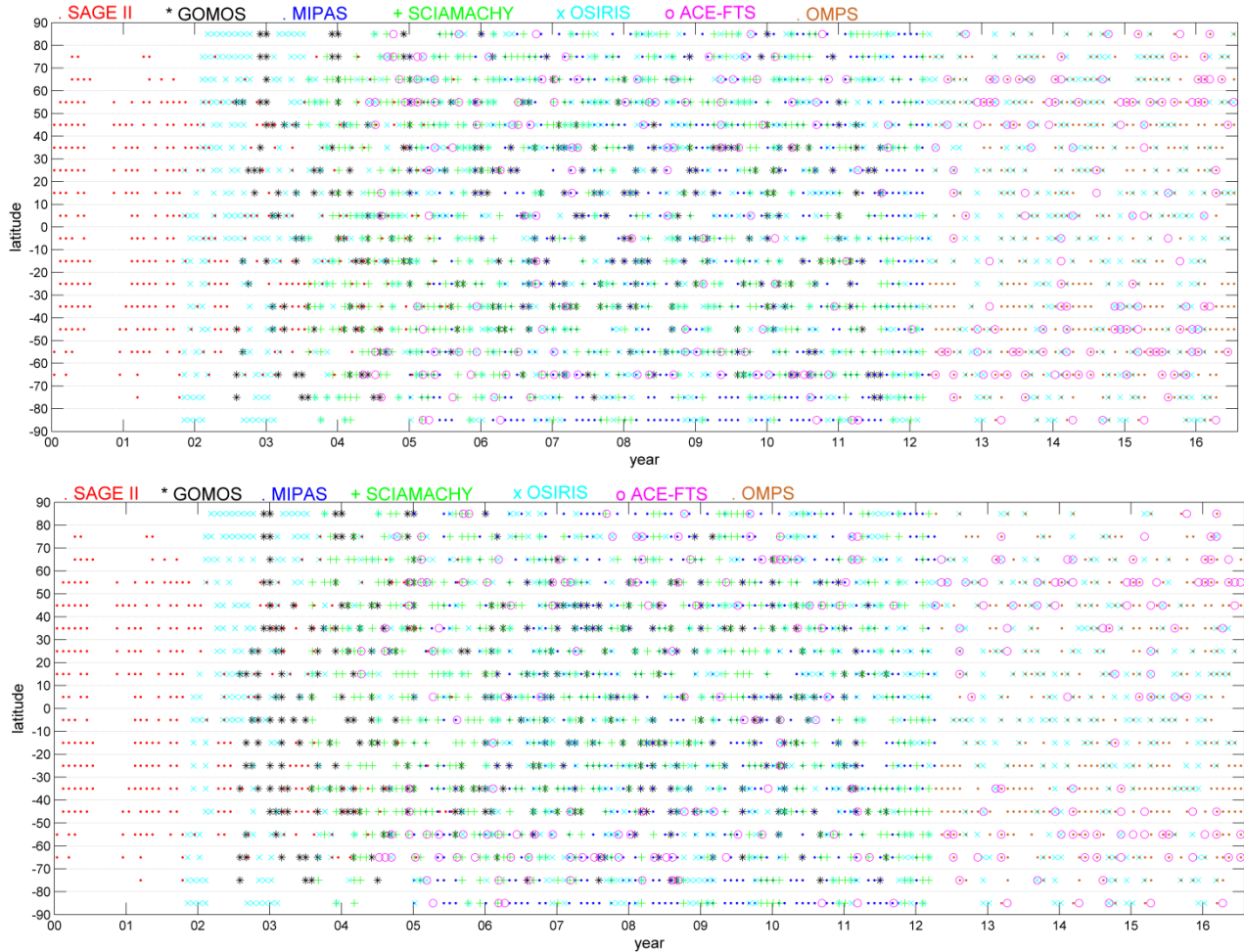
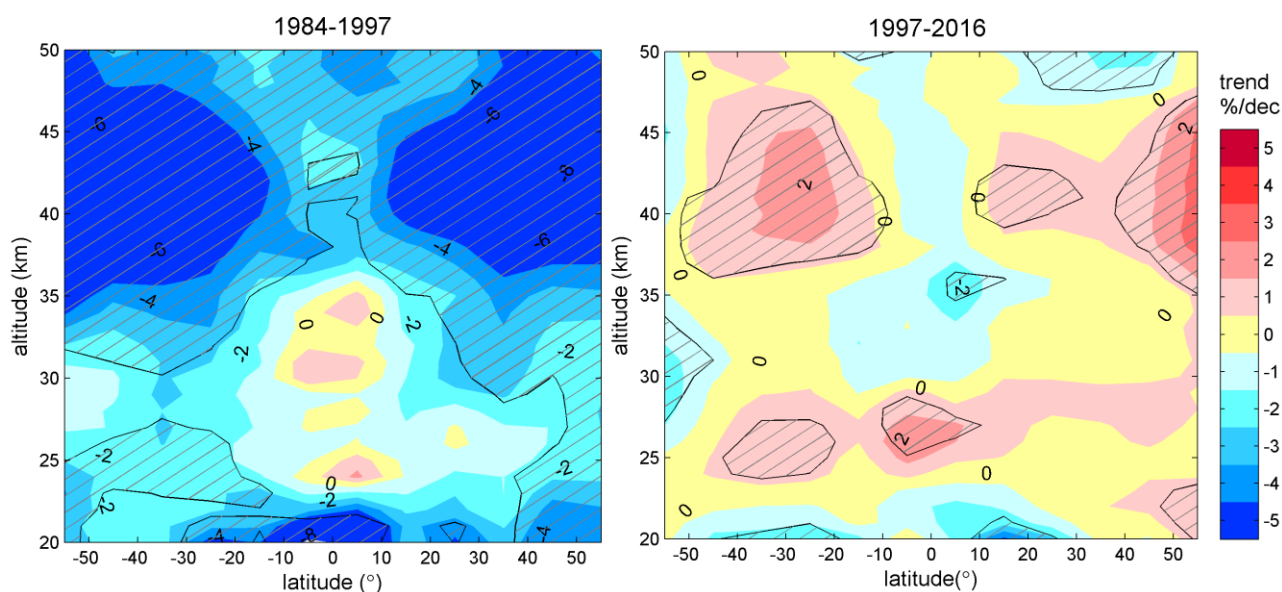


Figure S8. Colored markers indicate the instruments, which have anomalies within 1- $\sigma$  errorbar from the median value (merged anomaly), for 25 km (top) and 45 km (bottom).

## 3 Analyses of sensitivity of ozone trends

In this section, we present sensitivity analysis of ozone trends to:

- 1) Filtering of suspicious data;
- 2) Using only instruments, which retrieve ozone number density profiles on a geometric altitude grid.



**Figure S9.** The ozone trend in % per decade for different latitudes for 1984–1997 (left) and 1997–2016 (right). Shaded areas show regions where trends are statistically different from zero at the 95% level. In the merged dataset, the early period of SCIAMACHY and OMPS are not filtered.

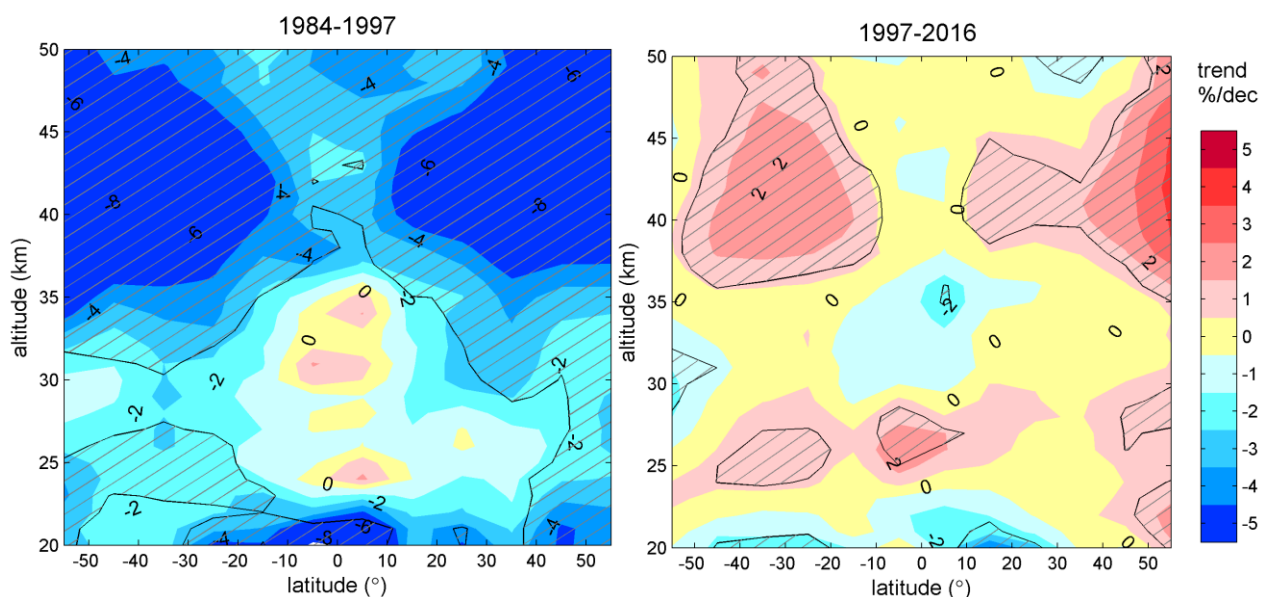


**Figure S10.** As Fig. S9, but MIPAS and ACE-FTS data are not used for the merged dataset.

For the first test, we created a version of the merged dataset in the same way but keeping the early periods of SCIAMACHY and OMPS operations and performed the same analysis. Keeping all data results in only very minor changes after 1997 are observed in ozone trends (mostly less than  $0.3 \text{ \% dec}^{-1}$ ), as illustrated by Fig. S9 (to be compared with Fig. 10 in the main paper).

For the second test, we created a version of the merged dataset without MIPAS and ACE-FTS data. This merged dataset contains only data that were retrieved in number density on geometric altitude grid. As expected, only minor changes in ozone trends after 1997 are observed (Fig. S10): they are less than  $0.3 \text{ \% dec}^{-1}$  below  $40^\circ$  latitude and are up to  $1 \text{ \% dec}^{-1}$  at latitudes  $40^\circ$ - $60^\circ$ , in both hemispheres.

## 4 From merged deseasonalized anomalies to merged ozone profiles

Computation of number density profiles from the merged deseasonalized anomalies is performed according to Eq.(4) in the paper: the seasonal cycle is restored. The best estimate of the amplitude of seasonal cycle is given by MIPAS measurements, because they provide all season pole-to-pole measurements with dense sampling. We take the absolute values of the seasonal cycle from SAGE II and OSIRIS in the overlapping period (which are very close to each other and also to GOMOS measurements), thus preserving the consistency in the dataset through the whole observation period. Technically, the seasonal cycle corresponding to the merged dataset is the MIPAS seasonal cycle, which is offset to the mean SAGE II and OSIRIS values. The illustrations of MIPAS, OSIRIS and SAGE II, and “merged” seasonal cycles are shown in Fig. S11.

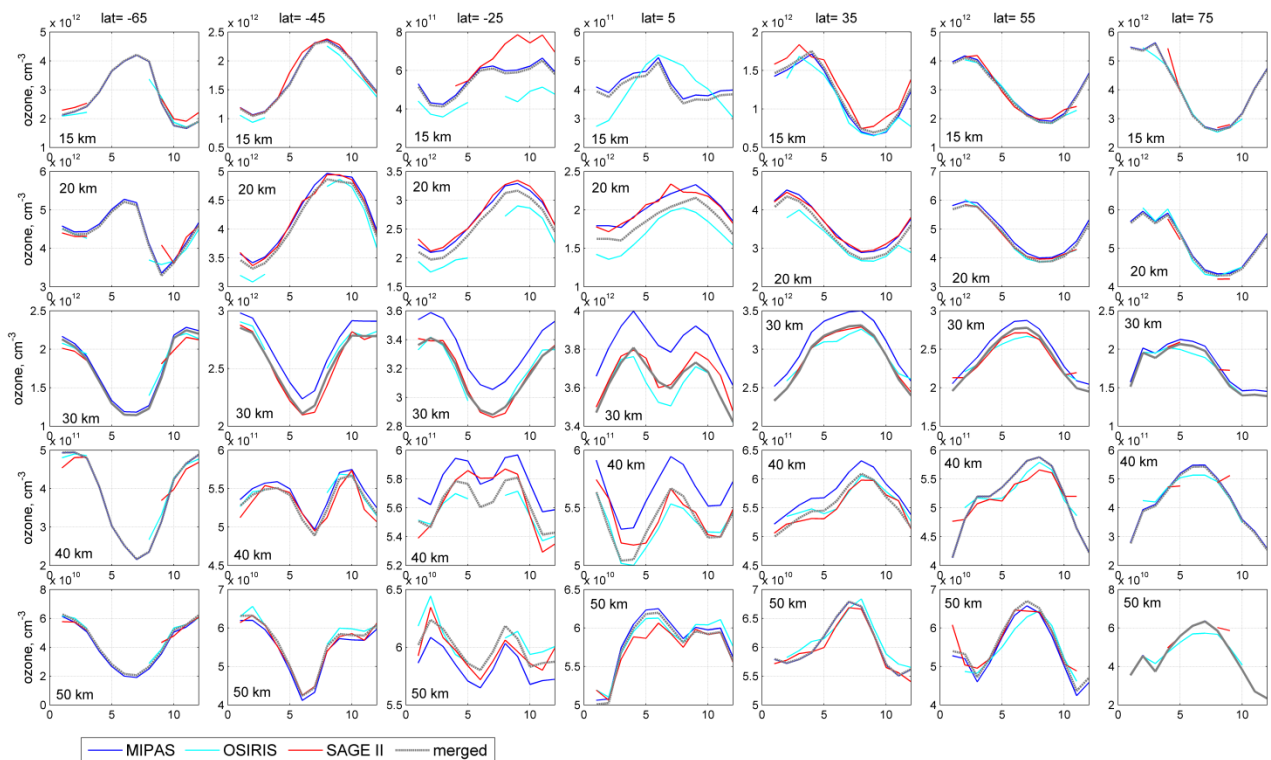


**Figure S11. Illustration of computing the seasonal cycle corresponding to the merged dataset (dashed grey lines). Colored lines: seasonal cycle estimates for MIPAS (blue), OSIRIS (cyan) and SAGE II (red).**

The examples of ozone number density time series from individual instruments and the merged SAGE-CCI-OMPS dataset are shown in Fig. S12, for the latitude band 50°-60° N.



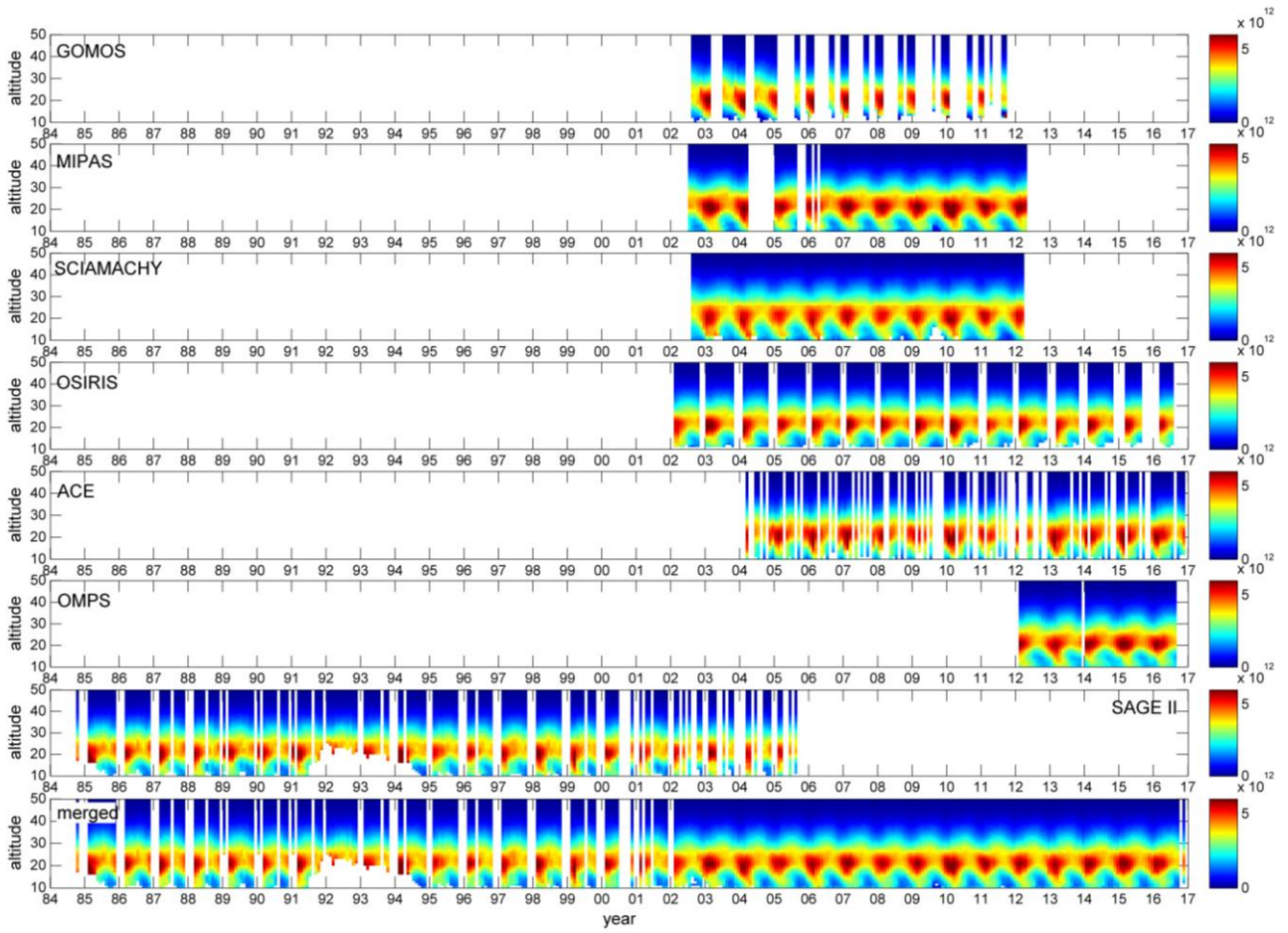


Figure S12. Ozone number density (color:  $\text{cm}^{-3}$ ), for individual datasets and the merged SAGE-CCI-OMPS dataset, for the latitude band  $50^{\circ}$ - $60^{\circ}$  N.